Published OnlineFirst September 10, 2015; DOI: 10.1158/1541-7786.MCR-15-0022

using the "Analyze particles" plugin (ImageJ software, imagej.nih.gov/ij/).

Apoptosis assay

Apoptosis level was measured based on the caspase-3 activity by utilizing the Ac-DEVD-AMC–specific caspase-3 substrate (Calbiochem). Upon addition of the caspase-3 substrate to the cell lysates, the fluorescence was detected at 460 nm on a microplate reader (Tecan). The results were normalized to the total protein concentration determined by Bradford Protein Assay.

Western immunoblot

Protein concentration of the whole-cell extracts was determined as described previously (30). Fifty micrograms of lysates were resolved by SDS-PAGE, transferred to PVDF membrane

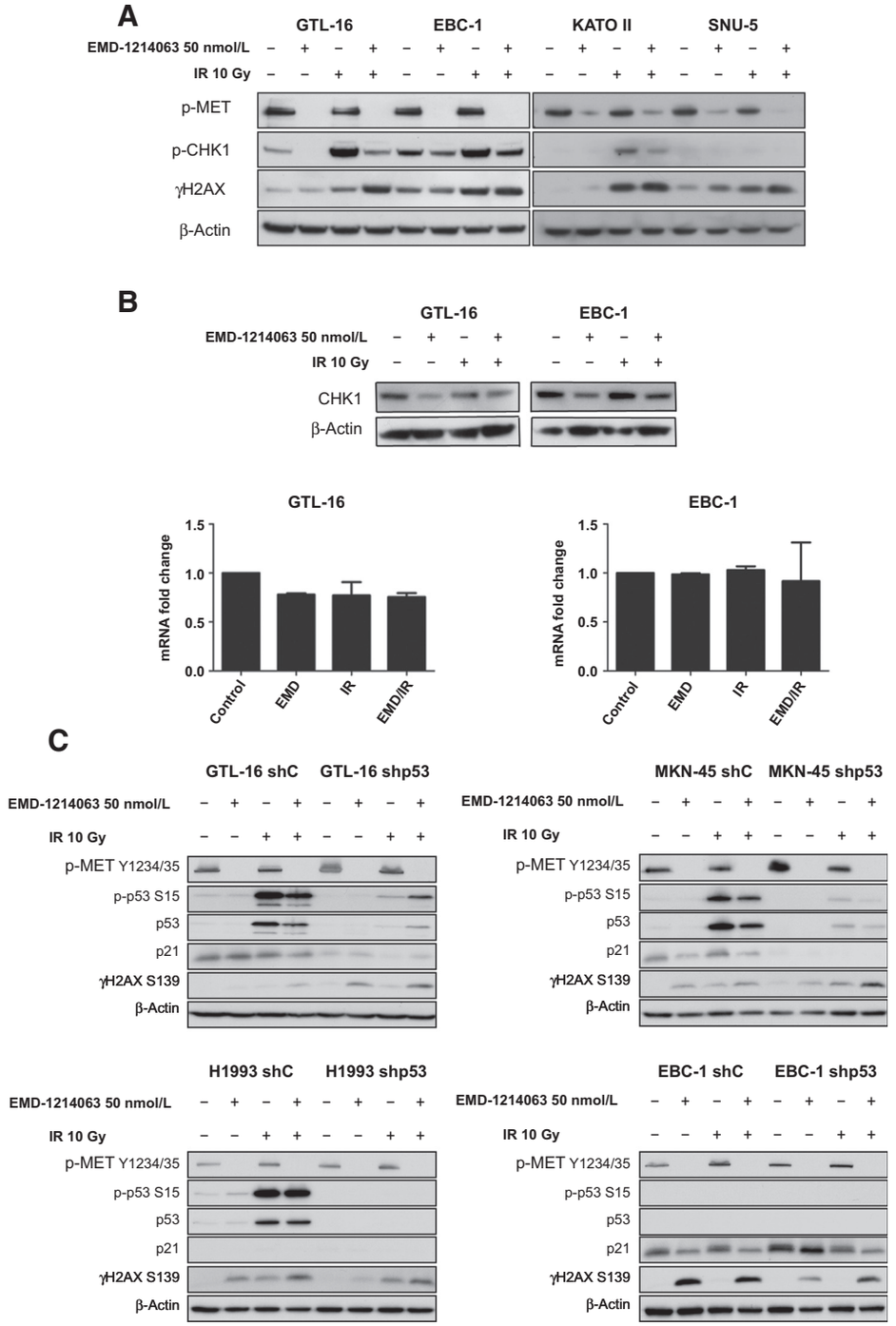

Figure 1.
Expression and activity of MET and DNA damage response effectors in MET-dependent cell lines. A, MET and CHK1 phosphorylation as well as γH2AX levels were determined in EMD-1214063 (16 hours), IR (30 minutes), or dually treated (16-hour drug treatment prior to IR) cells. Reduction of phospho-CHK1 Ser345 and elevated γH2AX Ser139 are detected in the presence of MET inhibitor. B, CHK1 total protein (top) and mRNA (bottom) levels were determined in GTL-16 and EBC-1 cells treated as in A. C, p53 knockdown efficiency was assessed in shp53 cells by measuring p53 expression, p53 phosphorylation (Ser15), and the expression of the p53 downstream target $p21^{CIP1}$ (CDKN1A) upon MET inhibition and IR using the identical experimental settings as in A. Increased γH2AX levels were detected in the GTL-16 and MKN-45 p53 knockdown cells compared with their corresponding wild-type p53-expressing control lines throughout the conditions, while this effect was absent in H1993 and EBC-1 cells harboring mutated p53. (Representing results from three independent experiments are shown. β-Actin was used as a loading control.)

Published OnlineFirst September 10, 2015; DOI: 10.1158/1541-7786.MCR-15-0022

(Life Technologies), and probed with primary antibody. Proteins were detected by enhanced chemiluminescence reagent (Amersham).

RNA isolation and real-time PCR

Total RNA was extracted from cultured cells using TRIzol reagent following the manufacturer's instructions (Roche). Reverse transcription of mRNA was performed using the Omniscript RT Kit (Qiagen). Quantitative PCR of CHK1 was done in a 7900HT Fast Real-time PCR System (Applied Biosystems) using a TaqMan assay (Applied Biosystems). The mean C_t was determined from triplicate experiments. mRNA levels were normalized to the level obtained for HMBS. Changes in expression were calculated using the $\Delta\Delta C_t$ method.

Cell cycle, mitotis, and DNA damage analyses

The cell-cycle distribution and the population of damaged and mitotic cells were determined by flow cytometry. Briefly, cells were fixed, stained with p-histone H3 (AlexaFluor488 conjugate), γH2AX (AlexaFluor647 conjugate), and propidium iodide (PI), and acquired on a flow cytometer (LSR II, BD). Cell cycle was evaluated by Dean/Jett/Fox algorithm using FlowJo Analysis Software.

Imaging flow cytometry

Imaging flow cytometry was used to analyze the genotoxicity in mitotic population by identifying micronuclei-containing cells. Briefly, fixed cells were labeled with phospho-histone H3 (AlexaFluor488 conjugate), phospho-histone H2AX (AlexaFluor647 conjugate), and DNA (DAPI). The samples were acquired on the ImageStreamX Mark II (Amnis, Millipore) and analyzed using IDEAS analysis software (Amnis, Millipore).

TCGA analysis

The cBioPortal for Cancer Genomics (http://www.cbioportal.org/public-portal/cross_cancer.do; refs. 31, 32) was used to obtain information on co-occurrence of *TP53* mutations and diverse *MET* alterations previously shown to result MET aberrant signaling (gene amplification, mRNA overexpression, and phosphorylation status) in different types of cancer.

Statistical analysis

Data were evaluated using two-tailored unpaired Student *t* test, *P* values of <0.05 were considered as significant (*, <0.05; **, <0.005; ***, <0.0005). Multiplicative systematic errors were eliminated for values obtained in cytotoxicity and caspase-3 assays as previously described (33).

Results

Targeting of MET by the small-molecule EMD-1214063 inhibits CHK1 activation

Previous work from our laboratory demonstrated the inhibition of the ATR-CHK1 signaling pathway in human gastric adenocarcinoma MET-overexpressing cell line GTL-16 as well as in NIH-3T3 mouse fibroblasts stably expressing the activating MET-mutated variant M1268T following treatment with anti-MET small-molecule PHA665752 (15). Here, an analogous decrease in the basal phosphorylation level of CHK1 on Ser345 (p-CHK1) was observed using a different selective MET tyrosine kinase inhibitor, EMD-1214063, in two MET-overexpressing cell lines, namely GTL-16 and the human NSCLC line EBC-1 (Fig. 1A). Moreover, the increase in CHK1 phosphorylation upon IR was also markedly impaired when this MET inhibitor was added prior to DNA damage. This effect of EMD-1214063 was also present in irradiated human gastric cancer cell lines KATO II and SNU-5, both of which overexpress the MET receptor and are classified as MET-dependent (34). Interestingly, prolonged MET inhibition by EMD-1214063 was accompanied also with a decrease in total amount of the CHK1 protein but not a decrease in its mRNA, indicating a potential MET signaling–related CHK1 regulation

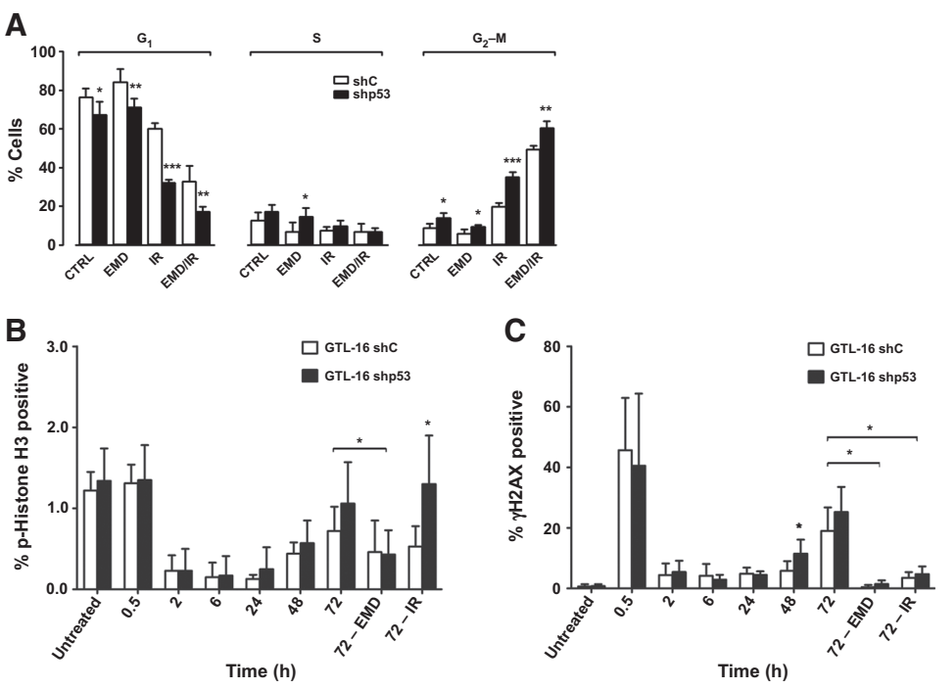

Figure 2.
Cell-cycle profile, mitotic population, and DNA damage in EMD-1214063 and IR-treated GTL-16 shC and shp53 lines. Cells were pretreated with the drug 1 hour prior to IR and analyzed 72 hours post-IR. A, cell-cycle analysis in shp53 cells exhibited significant reduction and increase in G_1 and G_2–M population, respectively, as compared with shC cells in all the conditions. B and C, time course study of mitotic index p-HH3 Ser10 and DNA damage marker γH2AX Ser139 in combined treated cells, in which their expression gradually increased up to 72 hours, especially in p53-knockdown GTL-16. For direct comparison, mitotic index p-HH3 Ser10 and DNA damage marker γH2AX Ser139 levels for EMD-1214063-treated (72 – EMD) and irradiated (72 – IR) cells at 72-hour time point are provided.

Published OnlineFirst September 10, 2015; DOI: 10.1158/1541-7786.MCR-15-0022

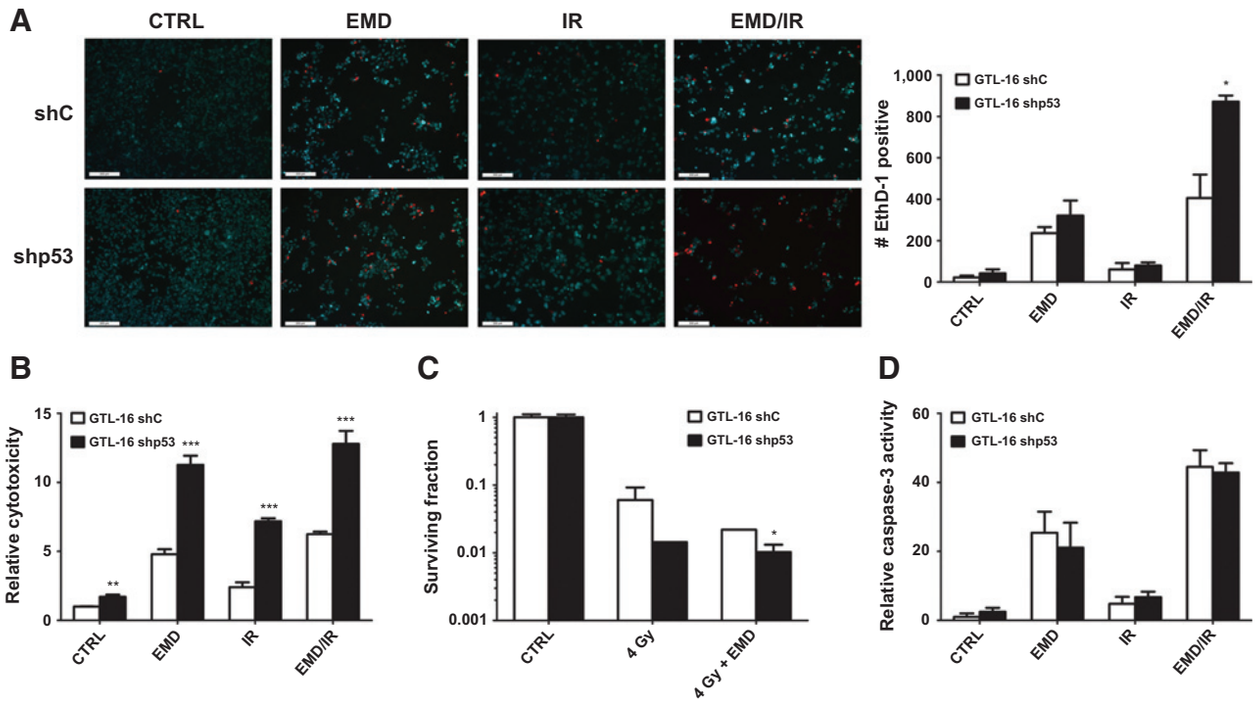

Figure 3.
GTL-16 control and p53 knockdown cells viability and toxicity. A, representative images (left) of viable and dead cells, calcium AM (green) or ethidium homodimer (red) positive, respectively, were acquired following EMD-1214063 (50 nmol/L), IR (10 Gy) and combination therapy (2 hours pretreatment with the anti-MET drug) after 72 hours (LIVE/DEAD). EMD/IR dual treatment in p53 knockdown (shp53) cells revealed decreased viability and enhanced cell death compared with control cells (shC). Quantification of three independent experiments is provided (right). B, cytotoxicity was quantified after 96 hours post-IR with or without 10 nmol/L MET inhibitor (1 hour treatment prior to IR) using CellTox Green Assay. p53 knockdown cells displayed significantly higher cell death in all conditions compared with control cells. C, clonogenic cell survival was assessed and scoring for colonies was performed 13 days after IR. GTL-16 shp53 cells showed decreased colony-forming capacity as compared with control (shC) cells upon IR (4 Gy) as well as upon the combined treatment [pretreatment by EMD-1214063 (50 nmol/L) 16 hours prior to IR]. D, relative caspase-3 activity was measured 72 hours post-IR in the presence or absence of EMD-1214063 (1 hour pretreatment prior to IR).

on a translational level (Fig. 1B). Because of the cross-talk and redundancy between CHK1 and CHK2 that have been reported in various cellular systems, we also investigated CHK2 activation status in GTL-16 and EBC-1 cells upon MET inhibition. However, unlike CHK1, the cellular levels and phosphorylation of CHK2 do not seem to be affected by EMD-1214063 (Supplementary Fig. S1).

Increased γH2AX expression upon MET inhibition in cells with compromised p53 function

As CHK1 plays a critical role in executing intra-S and G_2–M cell-cycle arrests upon DNA damage and MET inhibition compromises this checkpoint, we hypothesized whether cells deprived of the G_1 cell-cycle checkpoint (i.e., cancer cells lacking functional p53) would exhibit higher levels of DNA damage upon IR in combination with MET inhibition as compared with cells harboring intact p53 (20). To answer this question, various MET-dependent cell lines were treated with EMD-1214063. In these cells, MET phosphorylation at Tyr1234/1235 (Fig. 1A and C) as well as cell viability and proliferation remarkably decreased regardless of their p53 status (Supplementary Fig. S2A). Initially, we have shown that the increase of the DNA double-strand break marker Ser139 phosphorylated histone H2AX (γH2AX) upon irradiation, MET inhibition, and the combined treatment was also present across all these cell lines in a similar fashion as reported previously (Fig. 1A; ref. 15). This outcome indicates a slight tendency towards higher sensitivity to MET inhibition from higher γH2AX levels in p53-mutated (EBC-1 and SNU-5) in comparison with p53-proficient (GTL-16 and KATO II) cell lines (Supplementary Fig. S2B). To provide a solid link and to thoroughly investigate possible relation between the γH2AX levels and cellular p53 status, four different cell lines with deregulated MET activity, GTL-16, MKN-45, H1993, and EBC-1, were infected with shRNA against p53 through lentiviral delivery to generate isogenic pairs of scramble control (shC) and p53 knockdown (shp53) lines. GTL-16 and MKN-45 shC cells harboring wild-type p53 (35, 36) showed an upregulation in Ser15 phosphorylation of p53 (p-p53) as well as in total p53 levels following irradiation, while their shp53 counterparts displayed significantly lower levels of p-p53, total p53, and p21 in all the conditions (Fig. 1C). In addition, the reduction of p21 transactivation upon IR in GTL-16 shp53 compared with the parental line shown by the reporter gene assay further indicates the efficiency of p53 knockdown (Supplementary Fig. S2C). Moreover, an overall higher expression of γH2AX was detected in GTL-16 and MKN-45 shp53 cells as compared with their corresponding control lines (Fig. 1C). Importantly, this effect was not found in H1993 and EBC-1 isogenic pairs whose parental lines harbor mutated p53 (Fig. 1C; refs. 37, 38).

Published OnlineFirst September 10, 2015; DOI: 10.1158/1541-7786.MCR-15-0022

Enhanced accumulation of G_2–M population in EMD-1214063/IR–treated GTL-16 shp53 cells

We further evaluated the impact of MET inhibition and irradiation on cell-cycle distribution in GTL-16 shC and shp53 cells after 72 hours. While minor differences in the counts of S-phase cells were found both between the various conditions and the two cell lines, an overall decrease in G_1 population was detected in p53 knockdown as compared with control cells (Fig. 2A). This effect was particularly obvious when cells were exposed to irradiation alone or in combination with EMD-1214063. On the other hand, p53 knockdown cells displayed an elevated G_2–M-population as compared with control cells. Similar results were obtained using the selective CHK1 small-molecule inhibitor CHIR-124 as a single treatment and in combination with IR in the GTL-16 isogenic pair (Supplementary Fig. S3A). This indicates that the cells accumulate either in G_2- or in M-phase upon concomitant abrogation of both checkpoint regulators CHK1 and p53. It is important to note that CHIR-124 was used as an example of a direct CHK1 inhibition for comparison with the effects of the MET inhibitor EMD-1214063 that presumably also inhibits CHK1 signaling, albeit indirectly via inhibition of MET and downstream signaling.

Time-dependent increase in phospho-histone H3 and γH2AX expression following EMD-1214063/IR treatment in shp53 cells

The levels of histone H3 phosphorylation (p-HH3), a well-established marker for mitosis, were determined to quantify the cells in mitotic phase of the cell cycle. We evaluated the time-dependent counts of p-HH3- as well as γH2AX-positive cells following dual treatment with EMD-1214063 and irradiation for up to 72 hours. While the number of p-HH3–positive cells decreased after 2 hours, γH2AX-positive cells were highly abundant immediately after IR for a short period of time (Fig. 2B and C). Both DNA damage and mitotic marker–positive populations gradually increased from 24 hours on, in which shp53 line revealed consistently higher percentages of mitotic and γH2AX-positive cells as compared with the shC cells. Importantly, the observed increase in number of cells bearing DNA damage seems to be specifically related to the combined treatment as no such effect was present after 72 hours in cells treated by MET inhibition or IR alone (Fig. 2C).

EMD-1214063 combined with IR results in higher cytotoxicity in p53-deficient cells

To test whether cells with depleted p53 are more susceptible to cell death following EMD-1214063 and IR as compared with their p53-proficient counterparts, we aimed at simultaneous detection of viable and dead cell populations using Live/Dead Assay (Molecular Probes). Living cells, which were determined by the intracellular esterase activity, were monitored using fluorescence microscope together with dead cells that were stained with EthD-1. Our data show decreased number of viable and higher counts of EthD-1–positive GTL-16 shp53 cells treated with the MET inhibitor EMD-1214063 as compared with their

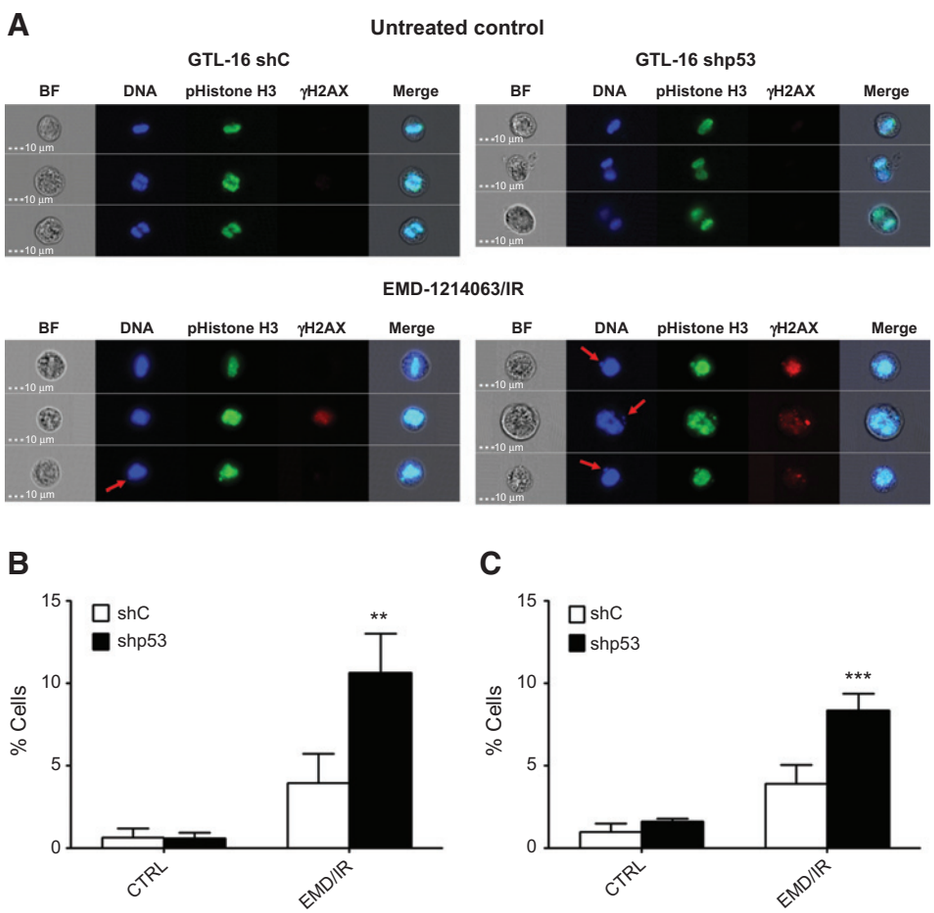

Figure 4.
Evaluation of genotoxicity in combined EMD-1214063 (10 nmol/L) and IR (10 Gy) treated GTL-16 cells after 72 hours. A, three representative single cell overlay images per condition of p-HH3 positive (green) cells that were stained with DAPI (blue) and γH2AX (red) are shown. While unstimulated cells underwent proper cell division, EMD/IR–treated cells displayed indication of micronuclei formation (red arrow) and γH2AX induction, predominantly in shp53 cells. B and C, sub-G_1 (DNA-fragmented) and >4n (polyploid) populations, respectively, were measured both in untreated and EMD/IR conditions by flow cytometry, revealing significant increase in both population in p53-knockdown variant as compared with the shC cells.

Published OnlineFirst September 10, 2015; DOI: 10.1158/1541-7786.MCR-15-0022

corresponding p53-proficient control cell line after 72 hours (Fig. 3A). These effects are further enhanced when EMD-1214063 treatment is combined with irradiation. In addition, the cytotoxicity mediated by these treatments was verified using CellTox Green Assay (Promega) that utilizes asymmetric cyanine-based dye that fluoresces upon binding to the dead cell DNA. Similar to the aforementioned results, the shp53 GTL-16 cells exhibited significantly higher levels of dead cells throughout the conditions, especially in the combined EMD-1214063/IR treatment (Fig. 3B). These observations have been further confirmed by significantly decreased clonogenic cell survival of shp53 GTL-16 as compared with p53-proficient cells when combining IR and MET inhibition (Fig. 3C). Similarly to the effects of EMD-1214063, the combination of CHIR-124 and IR synergistically increased the number of dead cells in shp53 GTL-16 cells, revealing more than 2-fold higher toxicity in p53 knockdown than in the control cells (Supplementary Fig. S3B).

Enhanced cytotoxicity in GTL-16 p53 knockdown cells is not mediated by apoptosis

We further raised the question whether the increase in cell death observed in shp53 cells as compared with shC cells upon the EMD-1214063/IR treatment is nevertheless of apoptotic nature. We therefore assessed the apoptotic response as one of the major cell death mechanisms by measuring the enzymatic activity of caspase-3. While irradiation slightly induced apoptosis, EMD-1214063 triggered more than 20-fold higher caspase-3 activity and this in both GTL-16 shC and shp53 cells (Fig. 3D). Furthermore, combined EMD-1214063/IR treatment synergistically increased the apoptotic event, in which the p53 knockdown cells showed similar levels of caspase-3 activity as the p53-proficient line. These observations indicate that although MET inhibition does induce apoptosis, this mode of cell death may not provide necessarily the rationale for increased cytotoxicity in cells with compromised p53 as compared with their isogenic cell line.

Increased genotoxicity in p53-depleted GTL-16 cells upon EMD-1214063/IR combined treatment

To shed more light on cell death mechanisms operative in p53 knockdown cells following combined MET inhibitor and IR treatment, morphologic and phenotypic analyses were performed in GTL-16 control and p53 knockdown lines upon the dual treatment. The γH2AX expression and DNA content were then evaluated in p-HH3–positive population that represents cells in mitotic phase. While proper cell divisions were observed both in untreated shC and shp53 cells, EMD-1214063/IR-treated population revealed aberrant mitosis accompanied by increased γH2AX expression, which was detected predominantly in the p53 knockdown cells (Fig. 4A). Moreover, the DNA staining implicates an indication of micronuclei formation in these cells suggesting the genotoxicity of the treatment. The quantification of polyploid (>4n) cells as well as the sub-G_1 fraction, which represents DNA fragmentation, substantiates enhanced susceptibility of shp53 cells to irradiation in combination with MET inhibition, suggesting the acquisition of mitotic aberrations as a potential cause of cell death following mitosis (Fig. 4B). In support of these findings, a decrease in cytotoxicity upon the combined EMD-1214063/IR treatment can be observed in shp53 cells once their mitotic progression is pharmacologically blocked using either nocodazole or the Polo-like kinase 1 inhibitor BI 2536 (Supplementary Fig. S4).

p53 status of MET-positive human tumor samples

To assess whether our findings are congruent with the molecular alterations found in human tumors, we analyzed the data sets from The Cancer Genome Atlas available at the cBioPortal for Cancer Genomics (http://www.cbioportal.org/public-portal/cross_cancer.do; refs. 31, 32) to match the genetic status of *TP53* with copy number alteration, mRNA expression, and reverse phase protein arrays (RPPA) data for *MET* in 5 different tumor types (Table 1). In this selected group of tumors, there was a statistically significant tendency towards co-occurrence of alterations in *TP53* and *MET* [as represented by odds ratio (OR) values significantly superior to 0]. *MET* gene amplification was generally uncommon (0%–4.65%), but tumors with *MET* amplification harbored *TP53* mutations in most lung and gastric adenocarcinomas (Table 1). mRNA overexpression was variable across tumoral entities (2.06%–16.09%), and co-occurrence of *TP53* mutations in such tumors was equally variable but tended to be higher than in the case of gene amplification. Finally, RPPA upregulation was relatively rare, and the levels of *TP53* mutations co-occurrence ranged between 6.67% and 28.57% (Table 1).

Discussion

Our previous work demonstrated a MET targeting–associated DNA damage response in MET-addicted cell lines by assessing increased γH2AX levels following exposure to the anti-MET–selective drug PHA665752 (15). Here, we report higher endogenous expression of γH2AX in p53 knockdown cells as well as in all tested p53-mutated lines in comparison with the wild-type p53 cells and elevated γH2AX in compromised p53 cells upon treatment with EMD-1214063, indicating genetic instability that potentially derives from the absence of the p53 function.

The phenotypic characteristics of elevated γH2AX background expression in p53 mutants as compared with the wild-type p53 cancer cells from a selected panel of NCI-60 tumor lines was previously reported (39). Although the retained γH2AX foci have been correlated with ultimate cell death that may arise from repair deficiency, replication stress, and telomere dysfunction, these expression levels may not be sufficient to predict the sensitivity towards radiation or chemotherapy (40).

Several studies have suggested the direct link between MET-driven tumors and their p53 status. For instance, a potential crosstalk between p53 and oncogenic MET activity was described by Furlan and colleagues, suggesting c-Abl as a signaling node that interconnects the MET and the p53 signaling pathway, in which wild-type p53 may contribute to tumorigenesis in interplay with oncogenic RTK system (36). However, most studies demonstrate that wild-type p53 exerts tumor-suppressing functions whereas compromised p53 is oncogenic. It has been proposed that esophageal epithelial cells harboring p53 mutation (R175H) gain oncogenic function and contribute to increased cell invasion via elevated MET activation (41). The high activity of the MET receptor and its association with enhanced motility, invasion, and scattering was correlated with the p53-dependent regulation of MET expression (42). Loss of wild-type p53 function due to mutations was shown to result in MET overexpression, increased MET signaling, receptor recycling, and consequently in progression to metastatic phenotypes. Moreover, the p53-mediated MET expression is facilitated both in miR-34a-dependent and

Published OnlineFirst September 10, 2015; DOI: 10.1158/1541-7786.MCR-15-0022

Table 1. Summary of coexpression data of *MET* and *TP53* (from cBioPortal for Cancer Genomics)

		MET							
Tumoral entity	**Reference (year)/no. of samples**	**Amplification (%)**	**mRNA upregulation (%)**	**RPPA upregulation (%)**	***TP53* mutations (%)**	***TP53* + *MET* amplification (%)**	***TP53* + *MET* mRNA upregulation (%)**	***TP53* + *MET* RPPA upregulation (%)**	**Association [OR (*P* value)]**
Lung adenocarcinoma	25079552 (2014)/230	3.48	16.09	0	49.13	62.5	75.67	—	0.673 (0.025)
Gastric adenocarcinoma	25079317 (2014)/258	4.65	13.57	NA	53.10	83.33	57.14	NA	0.675 (0.039)
Breast invasive carcinoma	23000897 (2012)/825	0	2.06	2.55	23.27	—	76.47	28.57	0.992 (0.001)
Glioblastoma multiforme	TCGA provisional data (accessed 03.21.2015)/611	2.95	5.73	2.13	16.37	22.2	25.71	23.08	0.713 (0.016)
Kidney renal clear cell carcinoma	23792563 (2013)/499	0.4	8.82	3.01	1.80	0	4.54	6.67	1.613 (<0.001)

Abbreviation: NA, data non available.

-independent manner via p53 (43–45). Taken together, the aggressive tumorigenic effect that associates with mutated p53, which has been also correlated with potential resistance to chemotherapeutic drugs, should be approached to improve cancer therapy outcome (46). As suggested by the current study, in the case of at least some MET-driven tumors, targeting of MET especially in p53-mutated background, may provide therapeutic benefit when a MET inhibitor is utilized concurrently among others, as a potential checkpoint abrogator.

As one of the essential steps in cellular DNA damage response, the activation of CHK1 prevents entry into mitosis in the presence of DNA lesions either at intra-S and/or at G_2–M transition. Thus, the concept of targeting CHK1 in tumors harboring deficient p53 for selective sensitization to radiation or to chemotherapeutic agents has been validated over the last decade using numerous CHK1 inhibitors (23–28, 47). Inhibition of CHK1 in various cancer types harboring p53 mutation including breast cancer, multiple myeloma, colon carcinoma, pancreatic cancer, and brain glioblastoma resulted in cell death mainly via mitotic catastrophe when simultaneously exposed to DNA damage. Currently, several CHK1 inhibitors (e.g., Sch 900776, GDC0425, GDC0575) are evaluated in clinical trials, highlighting the therapeutic advantage and benefits of a checkpoint abrogation approach in anticancer treatment (48–50).

Interestingly, a recent study showed that CHK1 inhibition potentiated the effect of chemotherapy in NSCLC-derived cancer stem cells and prevented tumor growth in mouse xenografts independently of p53 status (51). Moreover, Zenvirt and colleagues reported that p53-deficient cells are not susceptible to DNA damage following CHK1 inhibition to a greater extent than p53-proficient cells, but the p53 status rather determines the cell death mechanisms and survival. They have shown that while wild-type p53 cells underwent caspase-dependent apoptosis, p53-depleted counterpart resulted in cell death by mitotic catastrophe (52). This outcome is consistent with our current findings in respect to elevated apoptotic events in p53-proficient GTL-16 shC cells upon EMD-1214063 in combination with irradiation. On the other hand, our p53 knockdown line exhibited a comparable caspase-3 activation as well as significantly higher nuclear fragmentation and polyploidy following the combined therapy, which eventually lead to a reduced viability and enhanced cytotoxicity. The discrepancy in these studies may originate from the different targeted approaches and thus from corresponding mechanisms of action. While selective inhibition of CHK1 results mainly in defective DNA damage response, inactivation of the MET receptor particularly in MET-dependent tumors as used in our work induces growth arrest accompanied by the sensitization to DNA damage possibly via checkpoint abrogation. Yet, the long-term cell survival, clonogenicity, and the appropriate preclinical tumor model for this concept are still to be evaluated. Finally, the exact molecular mechanisms and the direct crosstalk between the MET signaling cascade and the DNA damage response machinery require a further extensive investigation.

In this study, we have further demonstrated the potential application of the selective small-molecule MET inhibitor EMD-1214063 as a mean to abrogate the intra-S and G_2–M checkpoint in MET-dependent tumors and have extended this concept by showing its radiosensitizing potential especially in cells with compromised p53 activity. Our results suggest that this targeted approach may overcome the resistance mechanism and its

Published OnlineFirst September 10, 2015; DOI: 10.1158/1541-7786.MCR-15-0022

associated poor clinical outcome that originates from deregulated p53 particularly in case of MET-driven tumors. As MET and p53 are aberrantly expressed or mutated, respectively, in numerous human malignant tumors and at significantly high frequencies, the concept of a possible synthetic lethality presented here as a mean of combining p53 deficiency and MET inhibition, thus depleting the cells of two important cell-cycle checkpoints (G_1 and G_2–M, respectively), may be of clinical relevance.

Disclosure of Potential Conflicts of Interest

A. Blaukat and F. Bladt are employees of Merck KGaA. No potential conflicts of interest were disclosed by the other authors.

Authors' Contributions

Conception and design: Y. Zimmer, M. Medová, K. Mikami
Development of methodology: M. Medová, K. Mikami, M.P. Tschan
Acquisition of data (provided animals, acquired and managed patients, provided facilities, etc.): K. Mikami, M. Medová, P. Francica, A. A. Glück, L. Nisa
Analysis and interpretation of data (e.g., statistical analysis, biostatistics, computational analysis): K. Mikami, M. Medová, Y. Zimmer, L. Nisa
Writing, review, and/or revision of the manuscript: K. Mikami, M. Medová, Y. Zimmer, D.M. Aebersold, A. Blaukat, F. Bladt, M.P. Tschan
Study supervision: Y. Zimmer, M. Medová

Acknowledgments

The authors thank Dr. W. Blank-Liss and B. Streit for their excellent technical support.

Grant Support

This study has been supported by Ruth & Arthur Scherbarth Stiftung grant (to M. Medová) and by the Swiss National Science Foundation (grant. no. 31003A_125394), Stiftung zur Krebsbekämpfung and Novartis Foundation (all to Y. Zimmer).

The costs of publication of this article were defrayed in part by the payment of page charges. This article must therefore be hereby marked *advertisement* in accordance with 18 U.S.C. Section 1734 solely to indicate this fact.

Received January 21, 2015; revised August 12, 2015; accepted August 24, 2015; published OnlineFirst September 10, 2015.

References

1. Watanabe S, Hirose M, Wang XE, Maehiro K, Murai T, Kobayashi O, et al. Hepatocyte growth factor accelerates the wound repair of cultured gastric mucosal cells. Biochem Biophys Res Commun 1994;199:1453–60.
2. Higuchi O, Nakamura T. Identification and change in the receptor for hepatocyte growth factor in rat liver after partial hepatectomy or induced hepatitis. Biochem Biophys Res Commun 1991;176:599–607.
3. Boccaccio C, Comoglio PM. Invasive growth: a MET-driven genetic programme for cancer and stem cells. Nat Rev Cancer 2006;6:637–45.
4. Trusolino L, Bertotti A, Comoglio PM. MET signalling: principles and functions in development, organ regeneration and cancer. Nat Rev Mol Cell Biol 2010;11:834–48.
5. Cecchi F, Rabe DC, Bottaro DP. Targeting the HGF/Met signalling pathway in cancer. Eur J Cancer 2010;46:1260–70.
6. Chen HH, Su WC, Lin PW, Guo HR, Lee WY. Hypoxia-inducible factor-1alpha correlates with MET and metastasis in node-negative breast cancer. Breast Cancer Res Treat 2007;103:167–75.
7. Zhang Y, Farenholtz KE, Yang Y, Guessous F, Dipierro CG, Calvert VS, et al. Hepatocyte growth factor sensitizes brain tumors to c-MET kinase inhibition. Clin Cancer Res 2013;19:1433–44.
8. Medova M, Aebersold DM, Zimmer Y. The molecular crosstalk between the MET receptor tyrosine kinase and the DNA damage response-biological and clinical aspects. Cancers 2013;6:1–27.
9. Bowers DC, Fan S, Walter KA, Abounader R, Williams JA, Rosen EM, et al. Scatter factor/hepatocyte growth factor protects against cytotoxic death in human glioblastoma via phosphatidylinositol 3-kinase- and AKT-dependent pathways. Cancer Res 2000;60:4277–83.
10. Skibinski G, Skibinska A, James K. Hepatocyte growth factor (HGF) protects c-met-expressing Burkitt's lymphoma cell lines from apoptotic death induced by DNA damaging agents. Eur J Cancer 2001;37:1562–9.
11. Fan S, Meng Q, Laterra JJ, Rosen EM. Ras effector pathways modulate scatter factor-stimulated NF-kappaB signaling and protection against DNA damage. Oncogene 2007;26:4774–96.
12. Fan S, Ma YX, Wang JA, Yuan RQ, Meng Q, Cao Y, et al. The cytokine hepatocyte growth factor/scatter factor inhibits apoptosis and enhances DNA repair by a common mechanism involving signaling through phosphatidyl inositol 3′ kinase. Oncogene 2000;19:2212–23.
13. Bhardwaj V, Cascone T, Cortez MA, Amini A, Evans J, Komaki RU, et al. Modulation of c-Met signaling and cellular sensitivity to radiation: potential implications for therapy. Cancer 2013;119:1768–75.
14. Toschi L, Janne PA. Single-agent and combination therapeutic strategies to inhibit hepatocyte growth factor/MET signaling in cancer. Clin Cancer Res 2008;14:5941–6.
15. Medova M, Aebersold DM, Blank-Liss W, Streit B, Medo M, Aebi S, et al. MET inhibition results in DNA breaks and synergistically sensitizes tumor cells to DNA-damaging agents potentially by breaching a damage-induced checkpoint arrest. Genes Cancer 2010;1:1053–62.
16. Medova M, Aebersold DM, Zimmer Y. MET inhibition in tumor cells by PHA665752 impairs homologous recombination repair of DNA double strand breaks. Int J Cancer 2012;130:728–34.
17. Lobrich M, Jeggo PA. The impact of a negligent G2/M checkpoint on genomic instability and cancer induction. Nat Rev Cancer 2007;7:861–9.
18. Gatei M, Sloper K, Sorensen C, Syljuasen R, Falck J, Hobson K, et al. Ataxia-telangiectasia-mutated (ATM) and NBS1-dependent phosphorylation of Chk1 on Ser-317 in response to ionizing radiation. J Biol Chem 2003;278:14806–11.
19. Toledo F, Wahl GM. Regulating the p53 pathway: in vitro hypotheses, in vivo veritas. Nat Rev Cancer 2006;6:909–23.
20. Ashwell S, Zabludoff S. DNA damage detection and repair pathways–recent advances with inhibitors of checkpoint kinases in cancer therapy. Clin Cancer Res 2008;14:4032–7.
21. Kim WY, Sharpless NE. The regulation of INK4/ARF in cancer and aging. Cell 2006;127:265–75.
22. Sherr CJ. Divorcing ARF and p53: an unsettled case. Nat Rev Cancer 2006;6:663–73.
23. Borst GR, McLaughlin M, Kyula JN, Neijenhuis S, Khan A, Good J, et al. Targeted radiosensitization by the Chk1 inhibitor SAR-020106. Int J Radiat Oncol Biol Phys 2013;85:1110–8.
24. Landau HJ, McNeely SC, Nair JS, Comenzo RL, Asai T, Friedman H, et al. The checkpoint kinase inhibitor AZD7762 potentiates chemotherapy-induced apoptosis of p53-mutated multiple myeloma cells. Mol Cancer Ther 2012;11:1781–8.
25. Ma CX, Cai S, Li S, Ryan CE, Guo Z, Schaiff WT, et al. Targeting Chk1 in p53-deficient triple-negative breast cancer is therapeutically beneficial in human-in-mouse tumor models. J Clin Invest 2012;122:1541–52.
26. Ma Z, Yao G, Zhou B, Fan Y, Gao S, Feng X. The Chk1 inhibitor AZD7762 sensitises p53 mutant breast cancer cells to radiation in vitro and in vivo. Mol Med Rep 2012;6:897–903.
27. Mitchell JB, Choudhuri R, Fabre K, Sowers AL, Citrin D, Zabludoff SD, et al. In vitro and in vivo radiation sensitization of human tumor cells by a novel checkpoint kinase inhibitor, AZD7762. Clin Cancer Res 2010;16:2076–84.
28. Tao Y, Leteur C, Yang C, Zhang P, Castedo M, Pierre A, et al. Radiosensitization by Chir-124, a selective CHK1 inhibitor: effects of p53 and cell cycle checkpoints. Cell Cycle 2009;8:1196–205.
29. Britschgi C, Rizzi M, Grob TJ, Tschan MP, Hugli B, Reddy VA, et al. Identification of the p53 family-responsive element in the promoter region of the tumor suppressor gene hypermethylated in cancer 1. Oncogene 2006;25:2030–9.

30. Zimmer Y, Vaseva AV, Medova M, Streit B, Blank-Liss W, Greiner RH, et al. Differential inhibition sensitivities of MET mutants to the small molecule inhibitor SU11274. Cancer Lett 2010;289:228–36.
31. Gao J, Aksoy BA, Dogrusoz U, Dresdner G, Gross B, Sumer SO, et al. Integrative analysis of complex cancer genomics and clinical profiles using the cBioPortal. Sci Signal 2013;6:pl1.
32. Cerami E, Gao J, Dogrusoz U, Gross BE, Sumer SO, Aksoy BA, et al. The cBio cancer genomics portal: an open platform for exploring multidimensional cancer genomics data. Cancer Discov 2012;2:401–4.
33. Echenique-Robba P, Nelo-Bazan MA, Carrodeguas JA. Reducing the standard deviation in multiple-assay experiments where the variation matters but the absolute value does not. PLoS One 2013;8:e78205.
34. Lai AZ, Durrant M, Zuo D, Ratcliffe CD, Park M. Met kinase-dependent loss of the E3 ligase Cbl in gastric cancer. J Biol Chem 2012;287:8048–59.
35. Sasaki Y, Negishi H, Idogawa M, Suzuki H, Mita H, Toyota M, et al. Histone deacetylase inhibitor FK228 enhances adenovirus-mediated p53 family gene therapy in cancer models. Mol Cancer Ther 2008;7:779–87.
36. Furlan A, Stagni V, Hussain A, Richelme S, Conti F, Prodosmo A, et al. Abl interconnects oncogenic Met and p53 core pathways in cancer cells. Cell Death Differ 2011;18:1608–16.
37. Fujita T, Kiyama M, Tomizawa Y, Kohno T, Yokota J. Comprehensive analysis of p53 gene mutation characteristics in lung carcinoma with special reference to histological subtypes. Int J Oncol 1999;15: 927–34.
38. Grabauskiene S, Bergeron EJ, Chen G, Thomas DG, Giordano TJ, Beer DG, et al. Checkpoint kinase 1 protein expression indicates sensitization to therapy by checkpoint kinase 1 inhibition in non-small cell lung cancer. J Surg Res 2014;187:6–13.
39. Yu T, MacPhail SH, Banath JP, Klokov D, Olive PL. Endogenous expression of phosphorylated histone H2AX in tumors in relation to DNA double-strand breaks and genomic instability. DNA Repair 2006;5:935–46.
40. Olive PL. Retention of gammaH2AX foci as an indication of lethal DNA damage. Radiother Oncol 2011;101:18–23.
41. Grugan KD, Vega ME, Wong GS, Diehl JA, Bass AJ, Wong KK, et al. A common p53 mutation (R175H) activates c-Met receptor tyrosine kinase to enhance tumor cell invasion. Cancer Biol Ther 2013;14:853–9.
42. Muller PA, Trinidad AG, Timpson P, Morton JP, Zanivan S, van den Berghe PV, et al. Mutant p53 enhances MET trafficking and signalling to drive cell scattering and invasion. Oncogene 2013;32:1252–65.
43. Hwang CI, Matoso A, Corney DC, Flesken-Nikitin A, Korner S, Wang W, et al. Wild-type p53 controls cell motility and invasion by dual regulation of MET expression. Proc Natl Acad Sci U S A 2011;108:14240–5.
44. Hwang CI, Choi J, Zhou Z, Flesken-Nikitin A, Tarakhovsky A, Nikitin AY. MET-dependent cancer invasion may be preprogrammed by early alterations of p53-regulated feedforward loop and triggered by stromal cell-derived HGF. Cell Cycle 2011;10:3834–40.
45. Menges CW, Kadariya Y, Altomare D, Talarchek J, Neumann-Domer E, Wu Y, et al. Tumor suppressor alterations cooperate to drive aggressive mesotheliomas with enriched cancer stem cells via a p53-miR-34a-c-Met axis. Cancer Res 2014;74:1261–71.
46. Strano S, Dell'Orso S, Di Agostino S, Fontemaggi G, Sacchi A, Blandino G. Mutant p53: an oncogenic transcription factor. Oncogene 2007;26:2212–9.
47. Walton MI, Eve PD, Hayes A, Valenti M, De Haven Brandon A, Box G, et al. The preclinical pharmacology and therapeutic activity of the novel CHK1 inhibitor SAR-020106. Mol Cancer Ther 2010;9:89–100.
48. Lee HJ, Muindi JR, Tan W, Hu Q, Wang D, Liu S, et al. Low 25(OH) vitamin D3 levels are associated with adverse outcome in newly diagnosed, intensively treated adult acute myeloid leukemia. Cancer 2014;120:521–9.
49. Gozzetti A, Defina M, Fabbri A. Myelosuppression after frontline fludarabine, cyclophosphamide, and rituximab in patients with chronic lymphocytic leukemia: analysis of persistent and new-onset cytopenia. Cancer 2014;120:451–2.
50. Karp JE, Thomas BM, Greer JM, Sorge C, Gore SD, Pratz KW, et al. Phase I and pharmacologic trial of cytosine arabinoside with the selective checkpoint 1 inhibitor Sch 900776 in refractory acute leukemias. Clin Cancer Res 2012;18:6723–31.
51. Bartucci M, Svensson S, Romania P, Dattilo R, Patrizii M, Signore M, et al. Therapeutic targeting of Chk1 in NSCLC stem cells during chemotherapy. Cell Death Differ 2012;19:768–78.
52. Zenvirt S, Kravchenko-Balasha N, Levitzki A. Status of p53 in human cancer cells does not predict efficacy of CHK1 kinase inhibitors combined with chemotherapeutic agents. Oncogene 2010;29:6149–59.